Journal of
Medical Genetics

ACBD5 deficiency causes a defect in peroxisomal very long-chain fatty acid metabolism

Journal:	*Journal of Medical Genetics*
Manuscript ID	jmedgenet-2016-104132.R2
Article Type:	Original Article
Date Submitted by the Author:	n/a
Complete List of Authors:	Ferdinandusse, Sacha; Laboratory Genetic Metabolic Diseases Falkenberg, Kim; AMC, Laboratory Genetic Metabolic Diseases Koster, Janet; AMC Mooyer, Petra; AMC Jones, Richard; Kennedy Krieger Institute van Roermund, Carlo; AMC, Laboratory Genetic Metabolic Diseases Pizzino, Amy; Children\'s National Health System, Department of Neurology Schrader, Michael; University of Exeter College of Life and Environmental Sciences, Biosciences Wanders, Ronald; Academic Medical Centre, Laboratory Genetic Metabolic Diseases Vanderver, Adeline; Childrens Natl Med Ctr Waterham, Hans; Academic Medical Center, Laboratory Genetic Metabolic Diseases (F0-222)
Keywords:	peroxisomal single enzyme deficiency, peroxisomal beta-oxidation, pexophagy, very long-chain fatty acids, acyl-CoA binding domain containing protein 5

ACBD5 deficiency causes a defect in peroxisomal very long-chain fatty acid metabolism

Sacha Ferdinandusse[1*#], Kim D. Falkenberg[1*], Janet Koster[1], Petra A. Mooyer[1], Richard Jones[2], Carlo W.T. van Roermund[1], Amy Pizzino[3], Michael Schrader[4], Ronald J.A. Wanders[1], Adeline Vanderver[3], Hans R. Waterham[1#]

[1]Laboratory Genetic Metabolic Diseases, Department of Clinical Chemistry, Academic Medical Center, Amsterdam, the Netherlands

[2]Kennedy Krieger Institute, Baltimore, Maryland, USA

[3]Department of Neurology, Children's National Health System, 111 Michigan Avenue, Northwest, Washington, DC 20010, USA

[4]College of Life and Environmental Sciences, Biosciences, University of Exeter, Exeter, Devon, UK

*Co-first authors
#Corresponding authors

Corresponding authors:

Sacha Ferdinandusse, PhD
Laboratory Genetic Metabolic Diseases, F0-220
Academic Medical Center
Meibergdreef 9
1105 AZ Amsterdam
The Netherlands
Phone: +31 205662485
Fax: +31 20 6962596
Email: S.Ferdinandusse@amc.nl

Hans R. Waterham, PhD
Laboratory Genetic Metabolic Diseases, F0-220
Academic Medical Center
Meibergdreef 9
1105 AZ Amsterdam
The Netherlands
Phone: +31 205665958
Fax: +31 20 6962596
Email: H.R.Waterham@amc.uva.nl

Word count: 4077

ABSTRACT

Background

Acyl-CoA binding domain containing protein 5 (ACBD5) is a peroxisomal membrane protein with a cytosolic acyl-CoA binding domain. Because of its acyl-CoA binding domain, ACBD5 has been assumed to function as an intracellular carrier of acyl-CoA esters. In addition, a role for ACBD5 in pexophagy has been suggested. However, the precise role of ACBD5 in peroxisomal metabolism and/or functioning has not yet been established. Previously, a genetic ACBD5 deficiency was identified in three siblings with retinal dystrophy and white matter disease. We identified a pathogenic mutation in *ACBD5* in another patient and studied the consequences of the ACBD5 defect in patient material and in ACBD5-deficient HeLa cells to uncover this role.

Methods

We studied a girl who presented with progressive leukodystrophy, syndromic cleft palate, ataxia and retinal dystrophy. We performed biochemical, cell biological and molecular studies in patient material and in ACBD5-deficient HeLa cells generated by CRISPR-Cas9 genome editing.

Results

We identified a homozygous deleterious indel mutation in *ACBD5*, leading to complete loss of ACBD5 protein in the patient. Our studies showed that ACBD5 deficiency leads to accumulation of very long-chain fatty acids (VLCFAs) due to impaired peroxisomal beta-oxidation. No effect on pexophagy was found.

Conclusions

Our investigations strongly suggest that ACBD5 plays an important role in sequestering C26-CoA in the cytosol and thereby facilitates transport into the peroxisome and subsequent beta-oxidation. Accordingly, ACBD5 deficiency is a novel single peroxisomal enzyme deficiency caused by impaired VLCFA metabolism and leading to retinal dystrophy and white matter disease.

KEYWORDS

Peroxisomal disorder, peroxisomal beta-oxidation, pexophagy, very long-chain fatty acids, acyl-CoA binding domain containing protein 5, peroxisomal single enzyme deficiency

INTRODUCTION

Peroxisomes play an important role in a number of essential metabolic pathways, including the biosynthesis of ether phospholipids and bile acids, the α- and β-oxidation of fatty acids, and the detoxification of glyoxylate and of reactive oxygen species generated in peroxisomes, i.e. hydrogen peroxide and superoxide.[1] Defects in human genes encoding peroxisomal proteins can result in different peroxisomal disorders with variable severity ranging from early lethality to subtle neurosensory abnormalities.[2, 3] The peroxisomal disorders are subdivided in two main classes: 1) the peroxisome biogenesis disorders, which include the Zellweger spectrum disorders and Rhizomelic chondrodysplasia punctata (RCDP) type 1 and 5, and 2) the single peroxisomal enzyme deficiencies.[3] In the first class multiple peroxisomal metabolic pathways are impaired, resulting in multiple metabolic abnormalities, whereas in the second class only the metabolic pathways, in which the defective enzyme participates, are impaired.[1] The clinical, biochemical and genetic spectrum of peroxisomal disorders is broad and still expanding. For example, recently, Heimler syndrome was recognized as a mild presentation of the Zellweger spectrum [4] and two novel types of RCDP (4 and 5) [5, 6] were identified. In this paper we report a novel peroxisomal single enzyme deficiency affecting the peroxisomal beta-oxidation of very long-chain fatty acids (VLCFAs), due to a deficiency of Acyl-CoA binding domain containing protein 5 (ACBD5).

ACBD5 is a peroxisomal membrane protein of 54.7-kDa with a C-terminal membrane-spanning region and an N-terminal cytosolic acyl-CoA binding domain. The peroxisomal localization of ACBD5 was established by proteomic analysis of purified peroxisomes from mouse kidney,[7] rat liver,[8, 9] and human liver [10] and confirmed by co-localization studies in cultured cells.[7, 8, 11] Because of its acyl-CoA binding domain, ACBD5 has been assumed to function as an intracellular carrier of acyl-CoA esters.[12] More recently, a role for ACBD5 in the degradation of peroxisomes, i.e. pexophagy, has been suggested mainly based on sequence similarity with the ATG37 protein of the yeast *Pichia pastoris*, which was implicated in this process.[11] However, the precise role of ACBD5 in peroxisomal metabolism and functioning had not been established.

Previously, a heterozygous missense variant in *ACBD5* was reported to cosegregate with autosomal dominant thrombocytopenia by Punzo et al.,[13] but a year later Pippucci et al. reported that the actual pathogenic mutations in this family and 7 additional families causing autosomal dominant thrombocytopenia are in the *ANKRD26* and not the *ACBD5* gene.[14] In 2013, exome sequencing of a large cohort of patients with retinal dystrophy identified three siblings with a genetic ACBD5 deficiency caused by a homozygous splice site mutation, but the pathogenic, physiological and functional consequences of the defect were not studied.[15] The retinal dystrophy was described as syndromic in the three siblings because of the combination with severe white matter disease and spastic paraparesis.

Here, we report in detail the clinical presentation of an ACBD5-deficient patient, who presented with progressive leukodystrophy associated with syndromic cleft palate, ataxia and retinal dystrophy. We furthermore show that the ACBD5 defect leads to accumulation of VLCFAs as a result of an impaired peroxisomal beta-oxidation of these fatty acids. Based on our findings, we postulate that ACBD5 functions as a peroxisomal membrane-bound receptor for VLCFA-CoAs.

MATERIALS & METHODS

Patient

The parents of the patient signed an informed consent approving the research.

Metabolic, biochemical and microscopical analyses

Concentrations of VLCFAs, phytanic and pristanic acid were determined in plasma as described in [16] and VLCFAs and C26:0 lysophosphatidylcholine (C26:0 lysoPC) were measured in cultured cells as described previously.[17, 18] Peroxisomal beta-oxidation of the VLCFA hexacosanoic acid (C26:0) and pristanic acid were measured as described.[19] A D3-C22:0 loading test was performed by loading cells for three days with deuterated (D3) C22:0 followed by fatty acid analysis with tandem mass spectrometry essentially as previously described,[20] but with D3-C22:0 instead of D3-C24:0.

Immunoblot analysis was performed with cell homogenates, which were separated by SDS-polyacrylamide gel electrophoresis, and subsequently transferred onto a nitrocellulose membrane using semidry blotting. We used rabbit polyclonal antibodies against ACBD5 (HPA012145, Sigma, directed against aa161-301, and AP9143a, Abgent, directed against aa69-98) at a 1:1000 dilution and mouse monoclonal antibodies against α-tubulin (T6199, Sigma) at a 1:2000 dilution or against β-actin (A5441, Sigma Alderich) at a 1:10.000 dilution. For visualization we used the secondary antibodies IRDye 800CW goat anti-rabbit and/or IRDye 680CW donkey anti-mouse with the Odyssey Infrared Imaging System (LI-COR Biosciences, Nebraska, USA).

For immunofluorescence microscopy, skin fibroblasts were cultured on cover slips to a confluency of approximately 60 to 70%. Cells were fixed and permeabilised with phosphate-buffered saline (PBS, Fresenius Kabi GmbH, Austria) solution containing 2% paraformaldehyde (Merck 8.18715.0100) and 0.1% Triton-X100 (BIO RAD 161-0407, 20'). After inactivating triton-X100 with 100 mM ammonium chloride (Merck 1.01145.1000, 10'), the cells were consecutively incubated with first and secondary antibodies and streptavidine-FITC complex (DAKO F 422) diluted in 1%BSA in PBS solutions for 5 minutes. The glass slides were fixed on objective slides with mounting medium Vectashield H1000 (Brunswick) and imaged using the fluorescence microscope Zeiss Axio Observer A1. We used primary antibodies against catalase (mouse monoclonal, Mab 17E10, own generation), ACBD5 (rabbit polyclonal, Sigma, HPA012145, diluted 1:500) and PMP70 (rabbit polyclonal, Zymogen, 718300, diluted 1:500), and as secondary antibodies Alexa Fluor® 555 Rabbit IgG (Z25305, ThermoFisher, diluted 1:500) or goat anti-mouse IgG antibody (DAKO, E433, diluted 1:200) or streptavidine-FITC complex (Bender Medsystems, diluted 1:200).

Cell culturing, transfections and functional complementation

Primary skin fibroblasts and HeLa cells were cultured in Ham's F-10 medium (Lonza, Basel, Switzerland) or Dulbecco's modified Eagle's medium (DMEM) with L-glutamine (Bio-Whittaker) supplemented with 10% fetal bovine serum (Bio-Whittaker), 25 mM HEPES buffer (BioWhittaker), 100 U/ml penicillin, 100 mg/ml streptomycin (Life Technologies), and 250 ng/ml fungizone (Life Technologies) in a humidified atmosphere of 5% CO_2 at 37^0C.

Transfection of HeLa cells was performed in 6-well plates using the jetPRIME® DNA transfection kit (Polyplus transfection, Illkirch-Graffenstaden, France) according to the manufacturer's instructions. Transfection of skin fibroblasts was performed using the AMAXA NHDF Nucleofector Kit (Lonza, Basel, Switzerland) according to the manufacturer's instructions (program U23).

For functional complementation we transfected patient's skin fibroblasts with the plasmid pcDNA3.1-hsACBD5, containing full-length human ACBD5 cDNA (1.5kb). The medium was changed 24 hours after transfection. For immunofluorescence microscopy, cells were imaged 3 days after transfection. For the D3-C22:0 loading test, D3-C22:0 was added to the medium one day after transfection and fatty

acid analysis was performed three days later. C26:0 lysoPC was measured in cell pellets four days after transfection.

Genetic analysis

Genomic DNA was isolated from skin fibroblasts using the NucleoSpin Tissue genomic DNA purification kit (Macherey-Nagel, Germany, Düren). All forward and reverse primers used for sequencing (available upon request) were tagged with a -21M13 (5'-TGTAAAACGACGGCCAGT-3') sequence or M13rev (5'-CAGGAAACAGCTATGACC-3') sequence, respectively. PCR fragments were sequenced in two directions using '-21M13' and 'M13rev' primers by means of BigDye Terminator v1.1 Cycle Sequencing Kits (Applied Biosystems, Foster City, CA, USA) and analyzed on an Applied Biosystems 3130x1 or 3730x1 DNA analyzer, following the manufacturer's protocol (Applied Biosystems, Foster City, CA, USA). *ACBD5* sequence data were compared with the reference *ACBD5* sequence (GenBank accession No. NM_145698.4) with nucleotide numbering starting at the first adenine of the translation initiation codon ATG.

Generation of ACBD5-deficient HeLa cells by Crispr-Cas9

The CRISPR-Cas9 genome editing technology as described by Ran 2013 was used to introduce a disruption of the *ACBD5* gene in HeLa cells.[21] To this end, two complementary oligonucleotides coding for a guide RNA upstream of a PAM site in exon 2 (5'-CGG, c.124_122) of the *ACBD5* gene were designed using the online CRISPR design tool (http://crispr.mit.edu/). The two oligo's were annealed and subsequently cloned into the pX458(-pSpCasq(BB)-2A-GFP) plasmid,[21] followed by Sanger sequencing of the insert to confirm the correct sequence. HeLa cells were transfected with 2 µg plasmid, and single GFP-positive cells were sorted into wells of a 96 wells plate using FACS flow cytometry (S800H Cell Sorter, Sony) as described.[21] After 3-4 weeks, DNA was isolated from the expanded single colonies and exon 2 of the *ACBD5* gene was PCR-amplified using Phire hot start II DNA polymerase (ThermoFisher Scientific, Waltham, MA, USA) according to the manufacturer's instructions and subsequently Sanger sequenced. We sequenced multiple clonal cells and found several with compound heterozygous mutations in *ACBD5*, suggesting that the HeLa cells were not aneuploid for the *ACBD5* gene. For subsequent studies we used cells (HeLaΔACBD5) that were apparent homozygous for the c.128insA mutation (p.V42fs*3), which was the most commonly found mutation among the clonal cells. Technically, however, we cannot exclude that these cells were hemizygous for the c.128insA mutation. The HeLaΔACBD5 cells were analyzed by immunoblotting to confirm the absence of ACBD5 protein and used for further experiments. The two putative off target regions of the *TLE6* and *DBNDD2* genes predicted by the online CRISPR design tool were sequenced, but did not contain mutations.

Pexophagy assay

To assess pexophagy in cells, we set up a similar Red-Green lysosome assay as described in [11, 22] using mCherry-GFP-SKL as peroxisomal reporter. Cells were cultured in live cell chambers (CELLview cell culture dishes (Greiner Bio-One, Kremsmünster, AT), which allowed to follow the development in time and prevented any influence of fixation on intracellular pH. Cells were transfected with 2 µg mCherry-GFP-SKL plasmid as described above. Twenty four hours after transfection the cells were either cultured in the presence of lysosomal protease inhibitors in order to prevent mCherry-GFP degradation in the lysosome (2 µM E-64 and 250 µM leupeptin (Enzo Life Sciences, East Farmingdale, NY, USA) or in the presence of the autophagy inhibitor 3-methyladenine (3-MA, Sigma-Aldrich, St. Louis, MO, USA).

Live cells were imaged with a Leica TCS SP8 filter-free spectral confocal microscope. Acquisition settings were adjusted to achieve a red and green signal of approximately equal intensity and

subsequently the same settings were used throughout the experiments. Red and green channel images were acquired simultaneously in order to prevent disturbances by peroxisomal movement. Excitation wavelengths of 489 or 587 nm were used for the green or red signal, respectively, and emission spectra were obtained at 499-550 nm or 597-671 nm, respectively (HyD SMD detectors, laser intensity 3%). The pixel size was between 42-44 nm. Ten to 40 images of cells per condition were acquired in 2 or 3 different areas of the live cell chambers; each image containing one single fibroblast or 1-4 HeLa cells.

Image processing was performed off-line using a commercial software package (MATLAB R2015a, The MathWorks Inc., Natick, MA, 2000). In summary, background noise was removed, peroxisomes were labelled and the red to green intensity for each of the peroxisomes was measured and analyzed. Background signals and non-peroxisomal signals were removed by processing the images of the red and green channel separately before merging them. To this end, we used multiple filters to remove the background signal, and additionally created a “mask”, which only selects peroxisomes. This mask consists exclusively of areas with high intensity of green and/or red signal. Areas with a minimum of 10 pixels were labelled as peroxisomes and used for quantification. The ratio of red to green signal (R/G) in each pixel was calculated, the number of pixels with an average R/G > 3 quantified (“red-only” pixels). For this study we defined fibroblasts with at least 20% “red-only” pixels as pexophagy-induced cells. In all HeLa cells the overall amount of “red-only” signal was below 20%, but peroxisomes undergoing pexophagy were clearly discernible by their bright red color. We defined HeLa cells as pexophagy-induced, when they displayed at least one of those bright red peroxisomes and quantified them manually (see also only online supplementary figure S3).

RESULTS

Case description

The patient, a girl, is one of three siblings from healthy consanguineous parents from the United Arab Emirates. Her sisters are both neurologically healthy, but one sister has been found to have a homozygous mutations in *MCR4* leading to morbid obesity. The patient was born full term by spontaneous vaginal delivery after a pregnancy complicated only by gestational diabetes managed with dietary changes. She was born with a cleft palate, for which correction was performed at six months, but appeared otherwise normal in the first months of life. At age seven months, she presented with abnormal eye movements and was diagnosed with retinal rod-cone dystrophy. She had delayed gains of motor skills; although she walked independently at one year, her gait was unsteady and she continued to need to hold on to objects to rise from the floor, which initially was attributed to her visual impairment. By two years of age, her gait had become progressively abnormal. She started to speak in sentences at the age of two and a half years and her cognitive function appeared relatively preserved.

By four years of age, however, it became apparent that her vocabulary was limited and she was dysarthric, despite normal hearing. She had developed a progressive microcephaly with facial dysmorphisms, including a tubular nose, hypotelorism, prominent ears, bilateral ptosis and rotatory nystagmus. Her motor dysfunction was marked,with a positive Gowers and proximal weakness, as well as increased extrapyramidal and pyramidal tone in her arms and legs. Her gait was wide-based with truncal titubation and waddling, and finger-nose-finger testing was remarkable for mild dysmetria. Over time, her gait became increasingly unbalanced. She developed greater difficulty with walking, descending stairs and decreased endurance with increased falling, and by the age of 9 years could walk only with two handed assistance or short distances with a walker. Brain MRI (see figure 1) at the age of 4 years revealed hypomyelination with diffuse T2 signal abnormality in deep white matter signal abnormalities with relative sparing of the subcortical U fibers. Signal abnormality was also seen to be involving the long tracts in the brainstem including the pyramidal tracts, the medial lemniscus, and the inferior cerebellar peduncles.

Peroxisomal investigations in blood and skin fibroblasts

Extensive laboratory testing including metabolic screening did not reveal clear abnormalities except for mildly increased plasma VLCFA levels (see Table 1). VLCFA analysis was repeated in a later sample and remained abnormal. In addition, C26:0 lysoPC and C26-acylcarnitine levels in bloodspot were increased. Other peroxisomal parameters in blood were normal (i.e. plasma phytanic acid, pristanic acid and pipecolic acid, and plasmalogens in erythrocytes). Based on the abnormal VLCFA profile a peroxisomal disorder was suspected, in particular acyl-CoA oxidase 1 (ACOX1) deficiency, affecting the first enzyme in peroxisomal VLCFA oxidation, or carriership of X-linked adrenoleukodystrophy (X-ALD). Both defects were excluded by Sanger sequencing of the genes involved (i.e. *ACOX1* and *ABCD1*). Subsequently, peroxisomal studies were performed in cultured primary skin fibroblasts of the patient. Immunofluorescence microscopy analyses with antibodies against the peroxisomal matrix protein catalase and the peroxisomal membrane proteins ABCD1 and ABCD3 revealed the normal presence of import-competent peroxisomes in fibroblasts of the patient. In addition, immunoblot analysis revealed normal peroxisomal processing of ACOX1 and peroxisomal thiolase, confirming normal peroxisome biogenesis in fibroblasts of the patient. VLCFA analysis showed that also in fibroblasts the C26:0 level was clearly increased with an increased C26:0/C22:0 ratio (see Table 1). In addition, C26:0 lysoPC was increased in fibroblasts showing that VLCFA levels in the phospholipid fraction are increased. To study the underlying cause of the C26:0 accumulation, peroxisomal fatty acid oxidation studies were performed with different radiolabeled substrates. Phytanic acid alpha-oxidation and pristanic acid beta-oxidation activities were normal compared to the reference values,

but C26:0 beta-oxidation was reduced (Table 1). The C26:0 beta-oxidation activity was decreased to 33% of the mean activity in the control fibroblasts within the same experiment. However, the activities of the enzymes involved in peroxisomal beta-oxidation of VLCFAs, i.e. ACOX1, D-bifunctional protein and Sterol carrier protein X, were not decreased when measured in a fibroblast homogenate. To further study VLCFA metabolism, we performed a loading study with deuterium labeled C22:0 (D3-C22:0). Fibroblasts were incubated with 30 µM D3-C22:0 for three days followed by fatty acid analysis with tandem-mass spectrometry. Both D3-C26:0 and D3-C28:0 levels were increased compared to the levels in the control fibroblasts analyzed in the same experiment showing increased chain elongation from the substrate D3-C22:0 most likely because of increased substrate availability due to impaired peroxisomal breakdown of D3-C22:0 (Table 2). Also unlabeled C26:0 levels were increased in this analysis with an increased C26:0/C22:0 ratio. The extent of the accumulation of the labeled and unlabeled VLCFAs was similar in fibroblasts of an X-ALD patient analyzed in the same experiment.

Table 1: Biochemical parameters in blood and fibroblasts of the patient

		Patient	Reference values
Blood	C26:0 lysoPC[a] (nmol/l)	166	29-72
	C26-carnitine[a] (µmol/l)	0.099	0.014-0.077
	C26:0[b] (µg/ml)	0.43	0.05-0.41
	C26:0/C22:0	0.025	0.002-0.018
	C24:0/C22:0	1.29	0.64-1.04
Fibroblasts	*VLCFAs (µmol/g)*		
	C22:0	3.01/4.40[c]	3.84-10.20
	C24:0	7.65/9.23[c]	7.76-17.66
	C26:0	1.07/1.14[c]	0.18-0.38
	C26:0/C22:0	0.35/0.26[c]	0.03-0.07
	C24:0/C22:0	2.54/2.10[c]	1.55-2.30
	C26:0 lysoPC	32	2-14
	Fatty acid oxidation activity (pmol/(hr.mg))		
	Phytanic acid alpha-oxidation	31	28-95
	Pristanic acid beta-oxidation	1086	748-975
	C26:0 beta-oxidation	437	1273-1431
	Activity of peroxisomal enzymes		
	DHAPAT (nmol/(2h.mg))	9.8	5.4-10.6
	ACOX1 (pmol/(min.mg))	285	74-206
	DBP hydratase (pmol/(min.mg))	143	115-600
	DBP dehydrogenase (pmol/(min.mg))	54	25-300

SCPx (pmol/(min.mg))	20	10-39

[a] measured in blood spot, [b] measured in plasma, [c] two independent measurements. Units are indicated between parentheses. Highlighted values are outside reference range

VLCFAs, Very long-chain fatty acids; DHAPAT, dihydroxy acetonephosphate acyltransferase; ACOX1, acyl-CoA oxidase 1; DBP, D-bifunctional protein; SCPx, sterol carrier protein X.

Table 2: D3-C22:0 loading test in fibroblasts

	Patient	X-ALD	Control 1	Control 2
D3-C28:0 (µmol/g)	0.22	0.13	*n.d.*	*n.d.*
D3-C26:0 (µmol/g)	1.53	1.86	0.67	0.24
D3-C24:0 (µmol/g)	12.87	19.93	12.75	11.02
C26:0 (µmol/g)	0.26	0.45	0.01	0.02
C26:0/C22:0	0.15	0.17	0.01	0.01
C24:0/C22:0	2.27	2.25	2.19	1.97

n.d., not detectable; X-ALD, X-linked adrenoleukodystrophy. Units are indicated between parentheses.

Genetic analysis and functional complementation studies

Because of the impaired peroxisomal beta-oxidation of C26:0 and the absence of mutations in *ACOX1* and *ABCD1*, we considered *ACBD5*, which encodes a peroxisomal membrane protein with a putative acyl-CoA binding domain, as a candidate gene. We performed molecular analysis of *ACBD5* by Sanger sequencing and identified a homozygous deleterious c.626-689_937-234delins936+1075_c.936+1230inv mutation (NM145698.4, see online supplementary figure S1). This mutation causes the deletion of exon 7 and 8 and is predicted to create a premature stop codon (p.D208Vfs*30). Both parents were heterozygous for this mutation, confirming homozygosity. Immunoblot analysis and immunofluorescence analysis with antibodies against ACBD5 demonstrated the absence of ACBD5 in fibroblasts of the patient (figure 2). To determine if the mutation in *ACBD5* was the underlying cause of the accumulation of VLCFAs in the patient, we transfected wild type *ACBD5* cDNA into the patient's fibroblasts followed by C26:0 lysoPC measurement and a D3-C22:0 loading test. ACBD5 expression was confirmed by immunoblot analysis (not shown). Four days after transfection the C26:0 lysoPC concentration had decreased from 29 in the mock-transfected cells to 18 µmol/g in the *ACBD5*-transfected cells (Table 3), which is just above the upper limit of the reference range in fibroblasts (2-14 µmol/g). Fatty acid analysis three days after loading the transfected cells with D3-C22:0 revealed a significant decrease in the levels of D3-C28:0 and D3-C26:0 compared to the mock transfected cells (Table 3). Also the level of unlabeled C26:0 was significantly reduced with a decrease in C26:0/C22:0 ratio. These results show that the impaired VLCFA metabolism in the patient's cells is caused by ACBD5 deficiency and can be rescued by introduction of wild type ACBD5.

Table 3: D3-C22:0 loading test and C26:0 lysoPC measurement after transfection of patient's fibroblasts with *ACBD5* cDNA

	mock	*ACBD5*

D3-C28:0 (µmol/g)	0.17 ± 0.01	0.05 ± 0.01*
D3-C26:0 (µmol/g)	2.20 ± 0.22	1.13 ± 0.13*
D3-C24:0 (µmol/g)	15.30 ± 1.51	12.52 ± 0.48
C26:0 (µmol/g)	0.35 ± 0.02	0.14 ± 0.06*
C26:0/C22:0	0.31 ± 0.13	0.15 ± 0.05
C24:0/C22:0	2.57 ± 0.96	2.60 ± 0.21
C26:0 lysoPC (µmol/g)	29	18

Fibroblasts were transfected with expression vector pcDNA3 (mock) or with pcDNA3 containing wild type *ACBD5* cDNA (*ACBD5*), n=3, mean ± SD. Units are indicated between parentheses. * indicates p≤0.005, Student t-test. D3, deuterated; lysoPC, lysophosphatidylcholine

Functional analysis of ACBD5 in HeLa cells

To confirm that ACBD5 deficiency causes VLCFA accumulation and to study the specific role of ACBD5 in peroxisome metabolism further, we introduced ACBD5 deficiency in HeLa cells by CRISPR-Cas9 genome editing. For our analysis we used HeLa cells which were apparent homozygous for a nucleotide insertion in exon 2 of *ACBD5* (c.128InsA, p.V42fs*3), which – similar to the patient's cells – resulted in the complete absence of the ACBD5 protein in the HeLa cells (HeLaΔACBD5) as confirmed by immunoblotting (see online supplementary figure S2). Peroxisomal investigations of these cells confirmed the findings in the primary patient's fibroblasts. The VLCFA profile was abnormal in HeLaΔACBD5 cells with an increased C26:0 level (0.18 µmol/g versus 0.053 in HeLa) and increased C26:0/C22:0 ratio (0.26 versus 0.07 in HeLa). C26:0 lysoPC was also increased in HeLaΔACBD5 cells (0.087 µmol/g versus 0.027 in HeLa). In addition, C26:0 beta-oxidation activity was reduced in HeLaΔACBD5 cells (583 pmol/(hr.mg protein) versus 971 in HeLa) and loading with D3-C22:0 resulted in accumulation of D3-C26:0 (0.34 µmol/g versus 0.15 in HeLa) just like in patient's fibroblasts. These results confirm that a deficiency of ACBD5 results in impaired peroxisomal VLCFA metabolism.

Role of ACBD5 in pexophagy?

Recently it has been suggested that, based on sequence similarity with ATG37 from the yeast *Pichia pastoris*, ACBD5 might play a role in pexophagy.[11] We studied this aspect in both the ACBD5-deficient patient's fibroblasts and HeLaΔACBD5 cells. To this end we used a previously described Red-Green lysosome pexophagy assay, in which a fusion protein composed of mCherry and GFP followed by a C-terminal peroxisomal targeting motif is expressed in cells. Expression of this fusion protein in cells predominantly results in yellow labelled peroxisomes whereas peroxisomes subject to pexophagy are "red-only" due to quenching of the green GFP fluorescence in the acidic environment of lysosomes.

We did not observe a difference in the level of pexophagy between control and ACBD5-deficient patient's fibroblasts upon expression of the reporter construct, while control cells treated with the autophagy inhibitor 3-MA showed a markedly lower number of pexophagy-induced cells (see figure 3 and online supplementary figure S3).We also performed the Red-Green lysosome assay in control and the ACBD5-deficient HeLa cells, a cell type used previously for this assay.[11, 22] Also in this cell system, the level of pexophagy in ACBD5-deficient HeLa cells was similar to the level in control HeLa

cells, while it was clearly decreased when the cells were treated with the autophagy inhibitor 3-MA (see figure 3 and online supplementary figure S3).

DISCUSSION

We report the identification and characterization of a patient with a deficiency of ACBD5 and show that ACBD5 deficiency is a novel single peroxisomal enzyme deficiency causing an impaired VLCFA metabolism. Screening of peroxisomal parameters in blood revealed an abnormal VLCFA profile and accumulation of C26:0 lysoPC. Furthermore, studies in the patient's fibroblasts revealed an impaired VLCFA metabolism as concluded from: 1) an abnormal VLCFA profile with increased concentration of C26:0 and increased C26:0/C22:0 ratio, 2) increased C26:0 lysoPC level showing an increased C26:0 concentration in the phospholipid fraction, 3) reduced peroxisomal C26:0 beta-oxidation activity but normal pristanic acid oxidation activity and 4) accumulation of D3-C26:0 and D3-C28:0 after loading fibroblasts with D3-C22:0 indicative of increased chain elongation due to increased substrate availability.

The ACBD5 defect in the patient was demonstrated by molecular analysis of the encoding gene and analysis of protein expression. The patient was homozygous for a deleterious c.626-689_937-234delins936+1075_c.936+1230inv mutation causing the absence of ACBD5 protein. The restoration of the biochemical phenotype of the patient's cells after transfection with wild type ACBD5, and the accumulation of C26:0 in the ACBD5-depleted HeLa cells confirmed that the impaired VLCFA metabolism in the patient is caused solely by ACBD5 deficiency.

ACBD5 is a peroxisomal membrane protein with a cytosolic acyl-CoA binding domain. Based on our findings in fibroblasts of the patient and the ACBD5-deficient HeLa cells we postulate that ACBD5 is involved in capturing C26-CoA in the cytosol through its acyl-CoA binding domain and presenting it to the VLCFA transporter ABCD1. ABCD1 then transports the C26-CoA into the peroxisome where it is beta-oxidized by the sequential action of the peroxisomal beta-oxidation enzymes ACOX1, D-bifunctional protein (DBP), sterol-carrier protein X (SCPX) and 3-ketoacyl-CoA thiolase. This postulated role of ACBD5 is supported by the fact that peroxisomal beta-oxidation activity of C26:0 in the ACBD5 patient's cells was reduced to a similar degree as observed in cells of X-ALD patients. In mitochondria, the acyl-CoA binding protein ACBP fulfills a similar function by binding palmitoyl-CoA and passing it on to carnitine palmitoyl-CoA transferase 1 (CPT1) for transport over the mitochondrial membrane to be beta-oxidized.[23]

ACBD5 was recently suggested to play a role in pexophagy.[11] It was hypothesized that the absence of ACBD5 would abrogate pexophagy and lead over time to an accumulation of peroxisomes. However, our studies in the patient's fibroblasts lacking ACBD5 and in HeLaΔACBD5 cells did not confirm an involvement of ACBD5 in pexophagy, at least in these cell types. In addition, we did not observe an obvious difference in peroxisome number between control and ACBD5-deficient cells. Instead our findings clearly showed that ACBD5 deficiency caused an impaired VLCFA metabolism.

VLCFA accumulation is not a biochemical abnormality exclusive to ACBD5 deficiency, but is also observed in other peroxisomal disorders, like X-ALD, ACOX1 and DBP deficiency and in Zellweger spectrum disorders (ZSDs).[3] In X-ALD, ACBD5 and ACOX1 deficiency, VLCFA accumulation is the only biochemical abnormality, whereas in DBP deficiency and ZSDs, multiple peroxisomal metabolic pathways are affected resulting in additional metabolic abnormalities. The patient presented with progressive leukodystrophy, ataxia, retinal dystrophy, cleft palate and facial dysmorphism, which are clinical symptoms that resemble those observed in patients with ACOX1 deficiency, but are different from X-ALD.[24] The underlying reason for this difference in clinical picture is unclear but could be due to a different tissue/cell type expression pattern of the proteins involved and a difference in the expression pattern of the proteins that can partly take over the function of the defective proteins (e.g. ABCD2 and ABCD3 in case of ABCD1 deficiency and ACOX2 in case of ACOX1 deficiency). Also the MRI abnormalities seen in this patient (Figure 1) are distinct from those seen in X-ALD or ZSDs.[25]

In a previous study aimed at determining the genetic causes of retinal dystrophy in a large cohort of patients by WES, a homozygous splice site mutation was identified in ACBD5 in three siblings with retinal dystrophy and white matter changes.[15] Although no further clinical details were provided, this suggests that the clinical presentation of ACBD5 deficiency is consistent. Since the focus of previous report was on exome sequencing, no metabolic investigations nor experiments to investigate the underlying pathological mechanism were presented. Our studies now show that ACBD5 deficiency belongs to the group of peroxisomal single enzyme deficiencies. This novel disorder should be included in addition to ACOX1 deficiency and X-ALD in the differential diagnostics in patients with clinical symptoms indicative of a peroxisomal disorder and an abnormal VLCFA profile.

Acknowledgements

We thank Lodewijk IJlst for his contribution.

Footnotes

SF and KDF contributed equally.

Contributors KDF, JK, PM, RJ and CWTR performed laboratory analyses. AP and AV were responsible for the clinical care of the patient, provided the patient's clinical information, and revised the manuscript. SF supervised the study and wrote the manuscript. HRW supervised the study and revised the manuscript. KDF, MS and RJAW revised the manuscript.

Funding Supported in part by funding through the Marie Curie Initial Training Networks (ITN) action to KDF, MS and HRW (FP7-2012-PERFUME-316723). MS is supported by the Biotechnology and Biological Sciences Research Council (BB/K006231/1; BB/N01541X/1).

Patient consent Obtained.

Competing interests None

Provenance and peer review Not commissioned; externally peer reviewed.

FIGURE LEGENDS

Figure 1. Brain MRI at the age of 4 years and 3 months (**A**). Please note the diffuse involvement of the deep white matter with abnormal T2 signal (**B**) and relatively more normal T1 signal (**C**) consistent with hypomyelination. The signal abnormalities demonstrate relative better myelination of the subcortical white matter (**D**, thin white arrow) and the anterior aspect of the corpus callosum (**A** and **B**). There is striking signal abnormality involving the posterior limb of the internal capsule, sparing the pyramidal tracts **(**dark dots in **B**)**.** The splenium of the corpus callosum is also strikingly affected (**A** thick white arrow and **B** thin white arrow). There are signal abnormalities of the long tracts of the brainstem, including the pyramidal tracts (**E** thin white arrow) and the medial lemniscus (**F** thin white arrow) in the pons and the superior (**E** dotted white arrow) and inferior cerebellar (**F** dotted white arrow) peduncles. There are no structural abnormalities of the brain, contrast enhancement or diffusion restriction abnormalities.

Figure 2. ACBD5 expression and localization in fibroblasts from the ACBD5-deficient patient and control subjects. (**A**) Immunoblot analysis of fibroblast lysates using antibodies against ACBD5 shows the absence of ACBD5 in the patient's cells. (**B**) Immunofluorescence microscopy of patient's and control fibroblasts using antibodies against catalase (left panels) and ACBD5 (right panels) confirms co-localization of catalase and ACBD5 in the control cells and the absence of ACBD5 in the patient's cells.

Figure 3. Pexophagy assay. (**A**) Cultured fibroblasts from the ACBD5-deficient patient and a control subject were transfected with mCherry-GFP-SKL and treated with lysosomal inhibitors (2 μM E-64, 250 μM leupeptin) 24 hours after transfection. Five days after transfection 10-40 cells were imaged in two to three independent experiments. Data presented as mean ratio (+ SD) of pexophagy-induced vs non-induced cells (See materials and methods for more details). For representative images see online supplementary figure S3. (**B**) Control HeLa cells and two HeLa-ΔACBD5 cell lines were transfected with mCherry-GFP-SKL and treated with lysosomal inhibitors (2 μM E-64, 250 μM leupeptin) 24 hours after transfection. Two days after transfection >35 cells were imaged in two independent experiments. Data presented as mean ratio (+SD) of pexophagy-induced cells vs non-induced cells (See materials and methods for more details). For representative images see online supplementary figure S3.

Supplementary figures

Figure S1. Schematic presentation of the homozygous c.626-689_937-234delins936+1075_c.936+1230inv mutation in the *ACBD5* gene of the patient. The upper graph depicts the complete *ACBD5* gene of the patient. The lower graph details the large intragenic deletion plus the original location of the small reverse complement intron 8 sequence insertion (striped part indicates reverse complement sequence). Arrows indicate the position of the sequencing primers used to determine the exact mutation.

Figure S2. ACBD5 expression in control HeLa and HeLa-ΔACBD5 cells. Immunoblot analysis of cell lysates using antibodies against ACBD5 shows the absence of ACBD5 in the HeLa-ΔACBD5 cells.

Figure S3. Representative images of fibroblasts and HeLa cells in the pexophagy assay. (**A**) mCherry-GFP-SKL transfected fibroblasts of the patient and control individuals (± autophagy inhibitor 3-MA) imaged five days after transfection. (**B**) mCherry-GFP-SKL transfected HeLa-ΔACBD5 cells and control HeLa cells imaged two days after transfection.

REFERENCES

1. Wanders RJ, Waterham HR. Biochemistry of mammalian peroxisomes revisited. *Annu Rev Biochem* 2006;75:295-332 doi: 10.1146/annurev.biochem.74.082803.133329.
2. Klouwer FC, Berendse K, Ferdinandusse S, Wanders RJ, Engelen M, Poll-The BT. Zellweger spectrum disorders: clinical overview and management approach. *Orphanet J Rare Dis* 2015;10:151 doi: 10.1186/s13023-015-0368-9.
3. Waterham HR, Ferdinandusse S, Wanders RJ. Human disorders of peroxisome metabolism and biogenesis. *Biochim Biophys Acta* 2015 doi: 10.1016/j.bbamcr.2015.11.015.
4. Ratbi I, Falkenberg KD, Sommen M, Al-Sheqaih N, Guaoua S, Vandeweyer G, Urquhart JE, Chandler KE, Williams SG, Roberts NA, El Alloussi M, Black GC, Ferdinandusse S, Ramdi H, Heimler A, Fryer A, Lynch SA, Cooper N, Ong KR, Smith CE, Inglehearn CF, Mighell AJ, Elcock C, Poulter JA, Tischkowitz M, Davies SJ, Sefiani A, Mironov AA, Newman WG, Waterham HR, Van Camp G. Heimler Syndrome Is Caused by Hypomorphic Mutations in the Peroxisome-Biogenesis Genes PEX1 and PEX6. *Am J Hum Genet* 2015;97(4):535-45 doi: 10.1016/j.ajhg.2015.08.011.
5. Baroy T, Koster J, Stromme P, Ebberink MS, Misceo D, Ferdinandusse S, Holmgren A, Hughes T, Merckoll E, Westvik J, Woldseth B, Walter J, Wood N, Tvedt B, Stadskleiv K, Wanders RJ, Waterham HR, Frengen E. A novel type of rhizomelic chondrodysplasia punctata, RCDP5, is caused by loss of the PEX5 long isoform. *Hum Mol Genet* 2015;24(20):5845-54 doi: 10.1093/hmg/ddv305.
6. Buchert R, Tawamie H, Smith C, Uebe S, Innes AM, Al Hallak B, Ekici AB, Sticht H, Schwarze B, Lamont RE, Parboosingh JS, Bernier FP, Abou Jamra R. A peroxisomal disorder of severe intellectual disability, epilepsy, and cataracts due to fatty acyl-CoA reductase 1 deficiency. *Am J Hum Genet* 2014;95(5):602-10 doi: 10.1016/j.ajhg.2014.10.003.
7. Wiese S, Gronemeyer T, Ofman R, Kunze M, Grou CP, Almeida JA, Eisenacher M, Stephan C, Hayen H, Schollenberger L, Korosec T, Waterham HR, Schliebs W, Erdmann R, Berger J, Meyer HE, Just W, Azevedo JE, Wanders RJ, Warscheid B. Proteomics characterization of mouse kidney peroxisomes by tandem mass spectrometry and protein correlation profiling. *Mol Cell Proteomics* 2007;6(12):2045-57 doi: 10.1074/mcp.M700169-MCP200.
8. Islinger M, Luers GH, Li KW, Loos M, Volkl A. Rat liver peroxisomes after fibrate treatment. A survey using quantitative mass spectrometry. *J Biol Chem* 2007;282(32):23055-69 doi: 10.1074/jbc.M610910200.
9. Kikuchi M, Hatano N, Yokota S, Shimozawa N, Imanaka T, Taniguchi H. Proteomic analysis of rat liver peroxisome: presence of peroxisome-specific isozyme of Lon protease. *J Biol Chem* 2004;279(1):421-8 doi: 10.1074/jbc.M305623200.
10. Gronemeyer T, Wiese S, Ofman R, Bunse C, Pawlas M, Hayen H, Eisenacher M, Stephan C, Meyer HE, Waterham HR, Erdmann R, Wanders RJ, Warscheid B. The proteome of human liver peroxisomes: identification of five new peroxisomal constituents by a label-free quantitative proteomics survey. *PLoS One* 2013;8(2):e57395 doi: 10.1371/journal.pone.0057395.
11. Nazarko TY, Ozeki K, Till A, Ramakrishnan G, Lotfi P, Yan M, Subramani S. Peroxisomal Atg37 binds Atg30 or palmitoyl-CoA to regulate phagophore formation during pexophagy. *J Cell Biol* 2014;204(4):541-57 doi: 10.1083/jcb.201307050.
12. Cohen Simonsen A, Bernchou Jensen U, Faergeman NJ, Knudsen J, Mouritsen OG. Acyl-coenzyme A organizes laterally in membranes and is recognized specifically by acyl-coenzyme A binding protein. *FEBS Lett* 2003;552(2-3):253-8.
13. Punzo F, Mientjes EJ, Rohe CF, Scianguetta S, Amendola G, Oostra BA, Bertoli-Avella AM, Perrotta S. A mutation in the acyl-coenzyme A binding domain-containing protein 5 gene (ACBD5) identified in autosomal dominant thrombocytopenia. *J Thromb Haemost* 2010;8(9):2085-7 doi: 10.1111/j.1538-7836.2010.03979.x.
14. Pippucci T, Savoia A, Perrotta S, Pujol-Moix N, Noris P, Castegnaro G, Pecci A, Gnan C, Punzo F, Marconi C, Gherardi S, Loffredo G, De Rocco D, Scianguetta S, Barozzi S, Magini P, Bozzi V,

Dezzani L, Di Stazio M, Ferraro M, Perini G, Seri M, Balduini CL. Mutations in the 5' UTR of ANKRD26, the ankirin repeat domain 26 gene, cause an autosomal-dominant form of inherited thrombocytopenia, THC2. *Am J Hum Genet* 2011;88(1):115-20 doi: 10.1016/j.ajhg.2010.12.006.

15. Abu-Safieh L, Alrashed M, Anazi S, Alkuraya H, Khan AO, Al-Owain M, Al-Zahrani J, Al-Abdi L, Hashem M, Al-Tarimi S, Sebai MA, Shamia A, Ray-Zack MD, Nassan M, Al-Hassnan ZN, Rahbeeni Z, Waheeb S, Alkharashi A, Abboud E, Al-Hazzaa SA, Alkuraya FS. Autozygome-guided exome sequencing in retinal dystrophy patients reveals pathogenetic mutations and novel candidate disease genes. *Genome Res* 2013;23(2):236-47 doi: 10.1101/gr.144105.112.
16. Vreken P, van Lint AE, Bootsma AH, Overmars H, Wanders RJ, van Gennip AH. Rapid stable isotope dilution analysis of very-long-chain fatty acids, pristanic acid and phytanic acid using gas chromatography-electron impact mass spectrometry. *J Chromatogr B Biomed Sci Appl* 1998;713(2):281-7.
17. Dacremont G, Cocquyt G, Vincent G. Measurement of very long-chain fatty acids, phytanic and pristanic acid in plasma and cultured fibroblasts by gas chromatography. *J Inherit Metab Dis* 1995;18 Suppl 1:76-83.
18. Ferdinandusse S, Ebberink MS, Vaz FM, Waterham HR, Wanders RJ. The important role of biochemical and functional studies in the diagnostics of peroxisomal disorders. *J Inherit Metab Dis* 2016 doi: 10.1007/s10545-016-9922-4.
19. Wanders RJ, Denis S, Ruiter JP, Schutgens RB, van Roermund CW, Jacobs BS. Measurement of peroxisomal fatty acid beta-oxidation in cultured human skin fibroblasts. *J Inherit Metab Dis* 1995;18 Suppl 1:113-24.
20. Kemp S, Valianpour F, Mooyer PA, Kulik W, Wanders RJ. Method for measurement of peroxisomal very-long-chain fatty acid beta-oxidation in human skin fibroblasts using stable-isotope-labeled tetracosanoic acid. *Clin Chem* 2004;50(10):1824-6 doi: 10.1373/clinchem.2004.038539.
21. Ran FA, Hsu PD, Wright J, Agarwala V, Scott DA, Zhang F. Genome engineering using the CRISPR-Cas9 system. *Nat Protoc* 2013;8(11):2281-308 doi: 10.1038/nprot.2013.143.
22. Deosaran E, Larsen KB, Hua R, Sargent G, Wang Y, Kim S, Lamark T, Jauregui M, Law K, Lippincott-Schwartz J, Brech A, Johansen T, Kim PK. NBR1 acts as an autophagy receptor for peroxisomes. *J Cell Sci* 2013;126(Pt 4):939-52 doi: 10.1242/jcs.114819.
23. Rasmussen JT, Faergeman NJ, Kristiansen K, Knudsen J. Acyl-CoA-binding protein (ACBP) can mediate intermembrane acyl-CoA transport and donate acyl-CoA for beta-oxidation and glycerolipid synthesis. *Biochem J* 1994;299 (Pt 1):165-70.
24. Ferdinandusse S, Denis S, Hogenhout EM, Koster J, van Roermund CW, L IJ, Moser AB, Wanders RJ, Waterham HR. Clinical, biochemical, and mutational spectrum of peroxisomal acyl-coenzyme A oxidase deficiency. *Hum Mutat* 2007;28(9):904-12 doi: 10.1002/humu.20535.
25. Vanderver A, Tonduti D, Schiffmann R, Schmidt J, van der Knaap MS. Leukodystrophy Overview. In: Pagon RA, Adam MP, Ardinger HH, et al., eds. GeneReviews(R). Seattle (WA), 1993-2016.

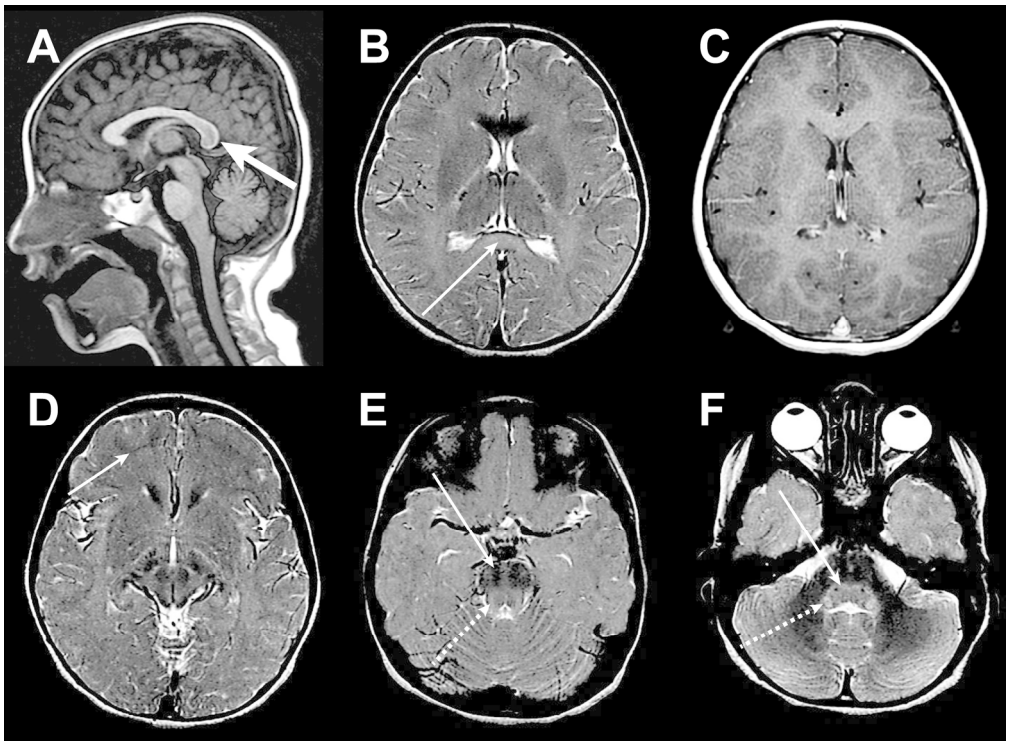

Figure 1. Brain MRI at the age of 4 years and 3 months.

179x131mm (300 x 300 DPI)

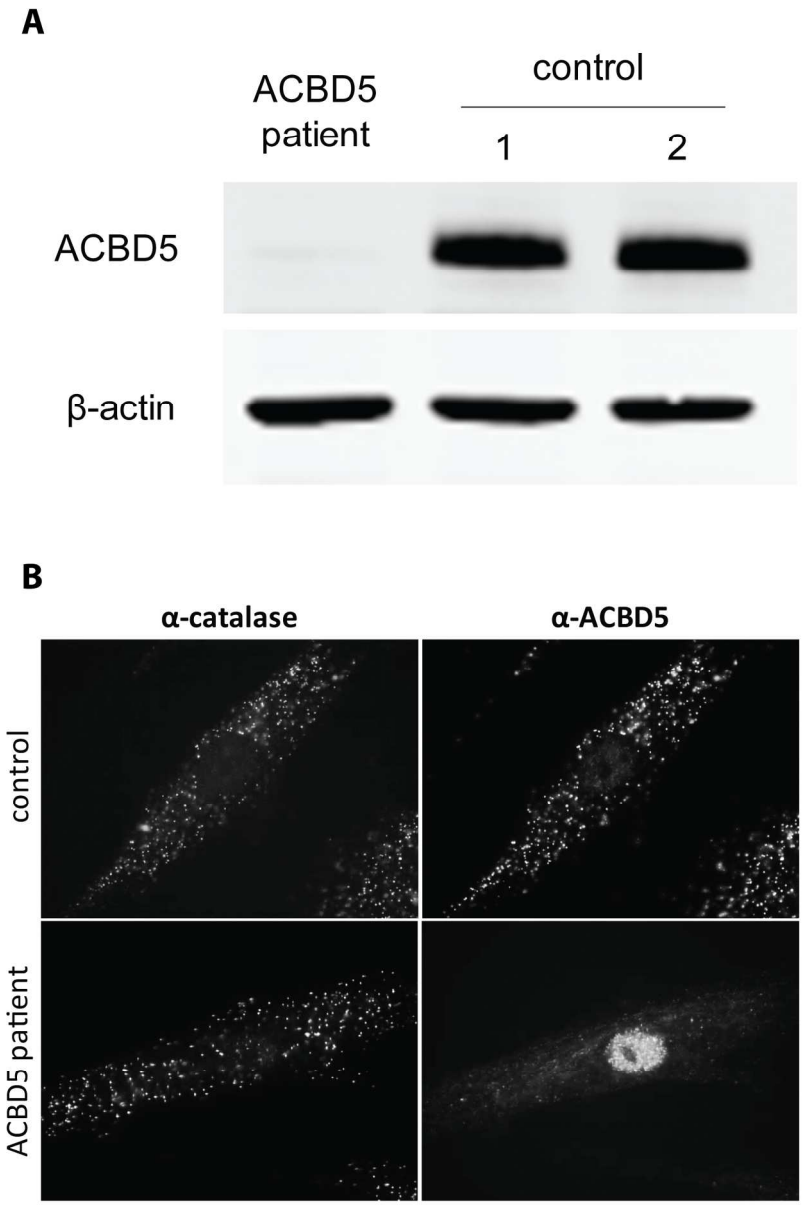

Figure 2. ACBD5 expression and localization in fibroblasts from the ACBD5-deficient patient and control subjects.

140x210mm (300 x 300 DPI)

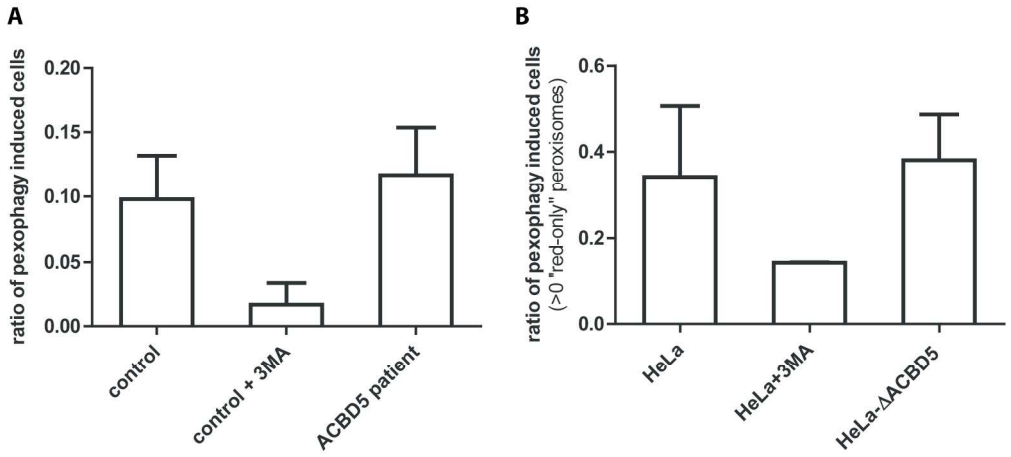

Figure 3. Pexophagy assay.

196x88mm (300 x 300 DPI)

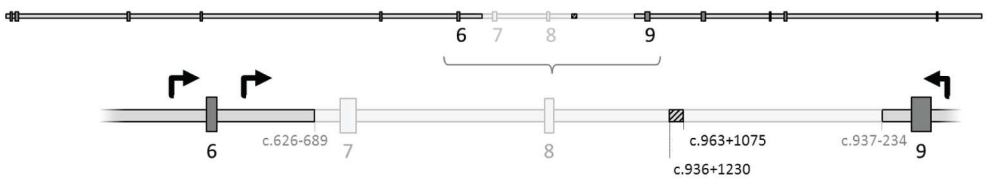

175x34mm (300 x 300 DPI)

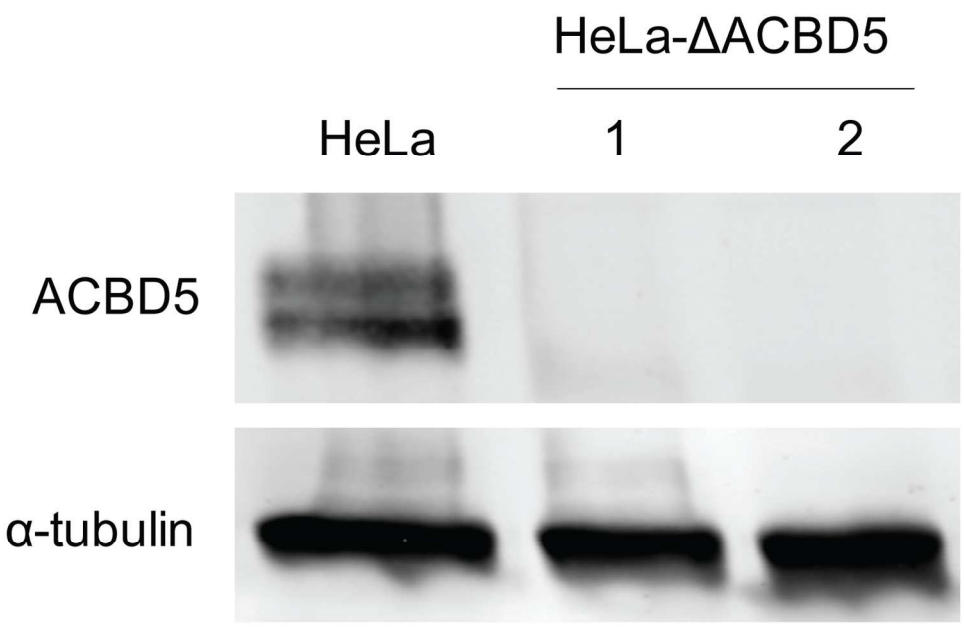

141x95mm (300 x 300 DPI)

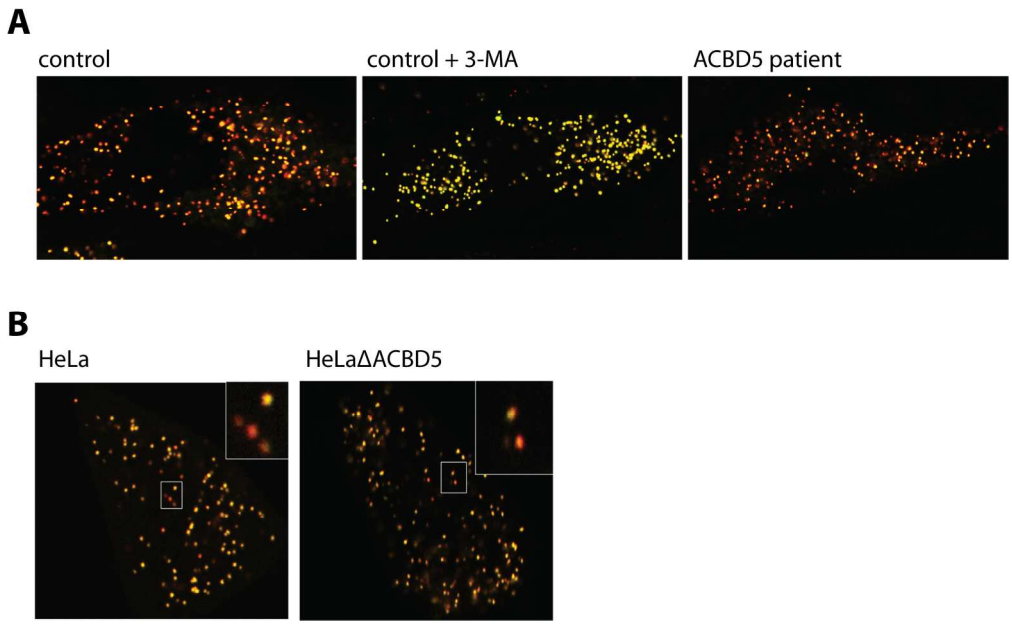

173x107mm (300 x 300 DPI)